

# Competing orders in the Dirac-like electronic structure and the non-linear sigma model with the topological term

Pouyan Ghaemi<sup>1,2</sup> and Shinsei Ryu<sup>1</sup>

<sup>1</sup>*Department of Physics, University of California at Berkeley, Berkeley, CA 94720, USA*

<sup>2</sup>*Materials Sciences Division, Lawrence Berkeley National Laboratory, Berkeley, CA 94720, USA*  
(ΩDated: November 14, 2018)

The Dirac-like electronic structure can host a large number of competing orders in the form of mass terms. In particular, two different order parameters can be said to be dual to each other, when a static defect in one of them traps a quantum number (or “charge”) of the other. We discuss that such complementary nature of the pair of the order parameters shows up in their correlation functions and dynamical properties when a quantum phase transition is driven by fluctuations of the one of the order parameters. Approaching the transition from the disordered (paramagnetic) side, the order parameter correlation function at the critical point is reduced, while such fluctuations enhance the correlation of the dual order parameter. Such complementary behaviors in the correlation function can be used to diagnose the nature of quantum fluctuations that is the driving force of the quantum phase transition.

## I. INTRODUCTION

Electrons in graphene<sup>1,2</sup>, one atom-thick flake of carbon, effectively behave as relativistic particles, governed by the (2+1)-dimensional Dirac Hamiltonian: the hopping of  $\pi$  orbitals on the honeycomb network of carbon atoms results in two Dirac points at the corners of the hexagonal Brillouin zone ( $\mathbf{K}_{\pm}$ ). The Dirac electronic structure by now is not an exclusive feature of graphene, but also appears on the surface of the (3+1)-dimensional  $\mathbb{Z}_2$  topological insulator<sup>3</sup> such as  $\text{Bi}_2\text{Se}_3$ <sup>4,5</sup> and  $\text{Bi}_2\text{Te}_3$ <sup>6,7</sup>, and in the quasi-two-dimensional organic conductor  $\alpha$ -(BEDT-TTF)<sub>2</sub>I<sub>3</sub><sup>8,9</sup>

In the Dirac electronic structure, a mass gap can be induced in the fermionic energy spectrum by a non-vanishing and uniform order parameter. In graphene, a variety of order parameters take on a form of such a mass term, including, e.g., the antiferromagnetism, valence bond solid (VBS), charge density wave (CDW), and superconductivity. Some of these mass terms are of topological nature, in the sense that when added they realize a topological insulator, such as the quantum Hall effect (QHE) or quantum spin Hall effect (QSHE), or a topological superconductor. (See, for example, Refs. 10–18, and references in Ref. 19).

Order parameters (mass terms) proximate to the Dirac electronic structure can be classified according to their algebraic properties. While they all anticommute with the Dirac kinetic term, as they induce a mass gap, they can either mutually commute or anticommute with each other (See below for more details). A set of mass terms which anticommute with each other do not compete, in the sense that one can adiabatically changes one order into another without closing a gap in the fermionic spectrum. Such mass terms can then be unified into a single multi-component order parameter, and each mass can be viewed as representing a different direction in the order parameter space. For example, the three antiferromagnetic orders (Néel orders) and the two different pat-

terns of the VBS do not compete and, at the level of the fermionic spectrum, can be integrated into a five-component (O(5)) vector.

When a topological defect is introduced in such a multi-component order parameter, midgap states appear in the massive Dirac energy spectrum. For example, for the case of the Néel-VBS 5-tuplet, one can create a vortex, say, in the  $x$  and  $y$  components of the Néel vector, or, in the two components of the VBS order parameters. A closer look at these topological defects and the midgap states reveals an interesting “duality” relation: A topological defect in the VBS order parameter supports two midgap states which carry a spin quantum number (i.e., form a doublet of  $S = 1/2$ ). On the other hand, a topological defect in the Néel vector, again, supports two midgap states which can be viewed as forming a doublet of the “valley pseudospin” degree of freedom. Here, by “valley pseudospin”, we mean the degree of freedom associated with the two Dirac cones (valleys) in the honeycomb lattice, and regard two valleys at  $\mathbf{K}_{\pm}$  as “pseudo spin up” and “pseudo spin down”, respectively. Such duality relation among order parameters can be found also in (3+1) dimensions.<sup>20</sup>

So far, the order parameters have been treated as a static background; they are either treated at a mean field level, or induced externally. Accordingly, topological defects are also introduced statically and by an external mean. In this paper, we turn our attention to the effects of electron correlations and on the dynamics of such order parameters.

While the vanishing density of states in the Dirac spectrum at the half-filling prevents order parameters from developing long-range order, when electron-electron interactions, say, are sufficiently strong, such orders can still be induced.

Here, an important implication of the duality relation between order parameters, found solely at the level of the fermionic energy spectrum, is the possibility of “deconfined” quantum criticality: I.e., a possible *contin-*

ous (second order) quantum phase transition between symmetry unrelated quantum phases, which is forbidden in the conventional Landau-Ginzburg framework.<sup>21</sup> The duality relation between different orders, i.e., a topological defect in one of the two carry a quantum number (“charge”) of the other, is a prerequisite for deconfined quantum criticality; with the duality, collapsing one phase by condensing defects automatically leads to the emergence of the other phase. I.e., they are connected through a continuous transition, and do not coexist.

The deconfined quantum criticality scenario has been investigated so far in the square-lattice quantum antiferromagnet; Indeed, a recent numerical study of the  $J$ - $Q$  model<sup>22,23</sup> observed a vortex-like texture of the VBS order parameter induced around a deficit of spin in the both columnar and plaquette VBS phases.

In this paper, including sufficiently strong short-range electron-electron interactions, we induce a mass gap in the Dirac spectrum dynamically (spontaneously), and study the structure of the resulting phase diagram and critical properties, with eyes on to the scenario of deconfined quantum criticality. In Sec. II, we introduce the Dirac Hamiltonian together with mass terms that represent order parameters of various kinds. The four-fermion interactions which result in a spontaneous generation of these order parameters are also introduced. One of our main results is the anomalous dimensions of the masses at the non-trivial critical point, Eqs. (17) and (19) in Sec. III. The detailed derivation of these are presented in Subsecs. III B-III D. We conclude in Sec. IV with our speculation on the two-parameter renormalization group (RG) flow in the non-linear sigma model (NL $\sigma$ M) with a topological term ( $\theta$ -term) in (2+1) dimensions.

## II. DIRAC HAMILTONIAN AND ORDER PARAMETERS

We start by describing the Dirac kinetic term of graphene Hamiltonian, which is represented by the single particle Hamiltonian  $\mathcal{H}_0(\mathbf{k})$  in momentum space as

$$\mathcal{H}_0(\mathbf{k}) = k_x \sigma_3 \otimes \tau_1 + k_y \sigma_3 \otimes \tau_2, \quad (1)$$

where  $\sigma_{1,2,3}$  and  $\tau_{1,2,3}$  are two independent sets of  $2 \times 2$  Pauli matrices, and we have set the Fermi velocity to be unity,  $v_F = 1$ . In graphene the Pauli matrices  $\tau_{x,y,z}$  act on the valley index whereas the Pauli matrices  $\sigma_{x,y,z}$  act on the sublattice index.

To describe several order parameters, including e.g., magnetic and superconducting order parameters, we introduce two more gradings, one for spin (represented by the Pauli matrices  $s_{1,2,3}$ ), and the other for particle-hole (represented by the Pauli matrices  $\mu_{1,2,3}$ ). (For more detailed description of the order parameters and the corresponding mass matrices entering in the Dirac Hamiltonian, see Ref. 19.)

### A. fermion mass terms in graphene

We now introduce mass terms in the Dirac Hamiltonian  $\mathcal{H}_0(\mathbf{k})$ . To discuss all possible duality relations among order parameters discussed in Ref. 19 in a unified fashion, let us start from a set of seven  $2^3 \times 2^3$  anticommuting hermitian matrices,

$$\begin{aligned} \xi_i \xi_j + \xi_j \xi_i &= 2\delta_{ij}, \quad i, j = 1, \dots, 7, \\ \text{with } \xi_7 &= i\xi_1 \xi_2 \cdots \xi_6. \end{aligned} \quad (2)$$

These matrices form a spinor representation of  $\text{SO}(7)$ . Two out of these seven matrices,  $\xi_{1,2}$ , can be used to form a Dirac kinetic Hamiltonian, whereas the remaining five matrices can be used as a mass matrix representing an order parameter:

$$\begin{aligned} \mathcal{H}(\mathbf{k}) &= \sum_{i=1}^2 k_i \xi_i + \sum_{i=3}^7 m_i \xi_i, \\ H &= \int d^2 k \Psi^\dagger \mathcal{H}(\mathbf{k}) \Psi. \end{aligned} \quad (3)$$

Here  $m_{i=3,\dots,7} \in \mathbb{R}$  represents a five-component order parameter;  $\Psi$  is a fermionic field operator which includes sublattice, valley, spin, and particle-hole gradings. For the cases of our interest, it turns out we can always take  $\Psi$  to be eight-component.<sup>19</sup> The imaginary-time Lagrangian is given by

$$\mathcal{L} = \Psi^\dagger \left( \partial_\tau + \sum_{i=1}^2 k_i \xi_i + \sum_{i=3}^7 m_i \xi_i \right) \Psi. \quad (4)$$

### B. four-fermion interactions

So far, we have been discussing order parameters  $m_i$  and their mass matrices  $\xi_i$  ( $i = 3, \dots, 7$ ) entering in the single-particle Dirac Hamiltonian, without asking their microscopic origin, i.e. microscopic interactions which can generate these orders dynamically. An interacting Hamiltonian which gives rise to these orders is:

$$\begin{aligned} H &= \int d^2 k \Psi^\dagger (\xi_1 k_x + \xi_2 k_y) \Psi \\ &\quad - \int d^2 r \sum_{a=3}^7 \frac{g_a}{2} (\Psi^\dagger \xi_a \Psi)^2, \end{aligned} \quad (5)$$

where  $g_a > 0$ . Such model can be designed on the lattice with extended Hubbard type interactions. With the Hubbard-Stratonovich (HS) transformation, these quartic interactions can be decoupled into channels, such as antiferromagnetic, superconducting, and VBS orders that we have discussed. If the coupling constants  $g_a > 0$  are large enough, we find a saddle point where these order parameters are non-zero.

While all coupling constants  $g_a$  can take, in principle, different values, below, let us first consider an interacting

Hamiltonian with  $g_a = g$  ( $a = 3, \dots, 7$ ),

$$H = \int d^2k \Psi^\dagger (\xi_1 k_x + \xi_2 k_y) \Psi - \int d^2r \frac{g}{2} \sum_{a=3}^7 (\Psi^\dagger \xi_a \Psi)^2. \quad (6)$$

This is an  $O(5)$  symmetric analogue of the (three-dimensional version of the) Gross-Neveu (GN) model.<sup>24</sup> The GN model with  $O(1) \simeq \mathbb{Z}_2$  internal symmetry and the chiral GN model with  $O(2) \simeq U(1)$  internal symmetry have been studied extensively, as a prototype model to discuss spontaneous chiral symmetry breaking. The corresponding Euclidean Lagrangian is

$$\mathcal{L} = \Psi^\dagger (\partial_\tau + \xi_1 k_x + \xi_2 k_y) \Psi - \frac{g}{2} \sum_{a=3}^7 (\Psi^\dagger \xi_a \Psi)^2. \quad (7)$$

We can successively break this  $O(5)$  symmetry down to  $O(4)$ , to  $O(3)$ , to  $O(2) \times O(2)$ , etc. In the following, in addition to the  $O(5)$  symmetric model, we consider  $O(4)$  and  $O(3)$  symmetric models as well. These models can be obtained from Eq. (5) by setting  $(g_3, g_{4,5,6,7}) = (0, g)$  (for the  $O(4)$  symmetric model) or  $(g_{3,4}, g_{5,6,7}) = (0, g)$  (for the  $O(3)$  symmetric model). In these cases, we can treat the remaining  $\xi$  matrices (i.e.  $\xi_3$  for the  $O(4)$  symmetric model or  $\xi_3$  and  $\xi_4$  for the  $O(3)$  symmetric model) as mass terms. Schematically,

$$H = \int d^2k \Psi^\dagger \left( \xi_1 k_x + \xi_2 k_y + \sum_{b \in M} m_b \xi_b \right) \Psi - \frac{g}{2} \int d^2r \sum_{a \in \bar{M}} (\Psi^\dagger \xi_a \Psi)^2, \quad (8)$$

where  $M = \emptyset, \{3\}, \{3, 4\}$ , for the  $O(5)$ ,  $O(4)$ , and  $O(3)$  symmetric models, respectively, and  $\bar{M}$  is the complement of  $M$ : We have added mass terms  $\sum_{b \in M} m_b \xi_b$  which are not generated spontaneously by the interactions. Rather, they are entering here as a parameter that changes the band structure of the single particle Hamiltonian. We will explore the phase diagram in terms of the coupling constant  $g$  as well as the masses  $m_b$  below.

When the coupling constant(s) is(are) large enough, the system is in an ordered phase. The phase diagram can be explored by saddle-point or mean field approximation. With the HS transformation,

$$\mathcal{L} = \Psi^\dagger \left( \partial_\tau + \xi_1 k_x + \xi_2 k_y + \sum_b m_b \xi_b + \sum_a v_a \xi_a \right) \Psi + \frac{1}{2g} \sum_a v_a^2. \quad (9)$$

If we freeze the dynamics of the HS fields ( $v_a$ ), we get the meanfield Hamiltonian discussed before. In the following, however, we are interested in the case where the HS fields are dynamical.

The  $O(N_\Sigma)$  ( $N_\Sigma = 3, 4, 5$  is the number of  $\Sigma_a$  matrices introduced below) symmetry of the problem can be seen

most clearly if we make the following change of basis in the fermionic path integral variables:

$$\begin{aligned} \gamma_0 &:= -\xi_3 \xi_4 \xi_5 \xi_6 \xi_7, & \gamma_1 &:= -i\gamma_0 \xi_1, & \gamma_2 &:= -i\gamma_0 \xi_2, \\ \Sigma_a &:= \gamma_0 \xi_{a+2}, & (a &= 1, \dots, N_\Sigma), \\ \bar{\psi} &:= \Psi^\dagger \gamma_0, & \psi &:= \Psi, \end{aligned} \quad (10)$$

wherein the Lagrangian in terms of the new variables is given by:

$$\mathcal{L} = \bar{\psi} \left( \partial_\mu \gamma_\mu + \sum_{a=1}^{N_\Sigma} v_a \Sigma_a \right) \psi + \frac{1}{2g} \sum_{a=1}^{N_\Sigma} v_a^2. \quad (11)$$

Here, the summation over space-time index  $\mu = 0, 1, 2$  is implicit, and we have switched off the masses  $m_b$  ( $b \in M$ ) momentarily. The merit of this change of variables is that it untangles rotations in the order parameter space and in the real space: the mass matrices ( $\Sigma_{a=1, \dots, N_\Sigma}$ ) and the matrices entering in the Dirac kinetic term ( $\gamma_{\mu=0, \dots, 2}$ ) are made mutually commuting,

$$[\gamma_\mu, \Sigma_a] = 0, \quad \forall \mu, a, \quad (12)$$

where  $\gamma$ s and  $\Sigma$ s form  $SO(3)$  and  $SO(N_\Sigma)$ , respectively,

$$\begin{aligned} \gamma_\mu \gamma_\nu + \gamma_\nu \gamma_\mu &= 2\delta_{\mu\nu}, & \mu, \nu &= 0, 1, 2, \\ \Sigma_a \Sigma_b + \Sigma_b \Sigma_a &= 2\delta_{ab}, & a, b &= 1, \dots, N_\Sigma. \end{aligned} \quad (13)$$

The  $O(N_\Sigma)$  rotation acting on the fermion fields  $\psi$  can be generated by unitary matrices  $\exp[iX^{ab}]$  where  $X^{ab} = [\Sigma_a, \Sigma_b]$ . With simultaneously rotating the  $N_\Sigma$ -component vector  $v_a$  appropriately, the Lagrangian is left invariant. Below, we will denote the dimension of  $\Sigma$ s and  $\gamma$ s by  $D_\Sigma$  and  $D_\gamma$ , respectively. In the above construction,  $D_\Sigma = D_\gamma = 8$ , while our calculations presented below are valid for any  $D_\Sigma$  and  $D_\gamma$ .

### C. meanfield phase diagram

To control the saddle point approximation (the mean field theory), and to prepare for the subsequent large- $N_f$  expansion, we generalize our Lagrangian to include  $N_f$  flavors of fermions. In the imaginary time formalism (the Euclidean signature), the large- $N_f$  generalized Lagrangian is then given by

$$\mathcal{L} = \sum_{i=1}^{N_f} \bar{\psi}_i \left( \gamma_\mu \partial_\mu + \sum_a v_a \Sigma_a + \sum_b m_b \Sigma_b \right) \psi_i + \frac{1}{2g} \sum_a v_a^2, \quad (14)$$

where  $\gamma_\mu$ s are Euclidean gamma matrices.

We now look for a spatially homogeneous and  $O(N_\Sigma)$  symmetric saddle point solution by setting

$$\mathbf{v}(x) = |v| \hat{\mathbf{n}}, \quad \hat{\mathbf{n}} \cdot \hat{\mathbf{n}} = 1. \quad (15)$$

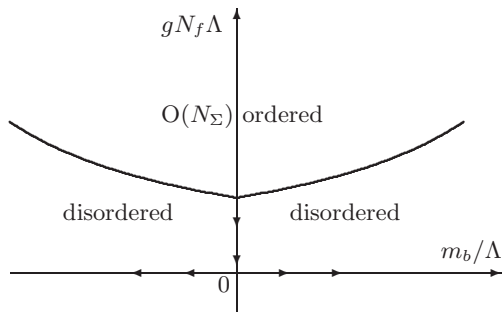


FIG. 1. The mean field phase diagram near the Dirac point.

When  $m_b = 0$  the self-consistency condition for  $|v|$  is given by

$$D_\gamma |v| \int^\Lambda \frac{d^3k}{(2\pi)^3} \frac{1}{k^2 + |v|^2} - \frac{|v|}{2N_f g} = 0. \quad (16)$$

Here we have introduced the ultra-violet (UV) cutoff  $\Lambda$  by hand.

The resulting mean-field phase diagram is depicted in Fig. 1, wherein we also include  $m_b$  ( $b \in M$ ): For sufficiently small  $g \ll 1/(N_f \Lambda)$ , there are two disordered phases where fermion fields are completely gapped by the mass  $m_{b \in M} \neq 0$ . They are separated by a phase boundary  $m_b = 0$ . In particular, when  $m_b$  represents the Kane-Mele mass term (QSHE mass term) it is a quantum phase transition separating the trivial band insulator and the topological (QSH) insulator. For sufficiently large  $g \gg 1/(N_f \Lambda)$ ,  $O(N_\Sigma)$  symmetry is spontaneously broken. The arrows in Fig. 1 indicates the infra-red (IR) renormalization group (RG) flow. Just at the non-interacting Dirac point, four fermion interactions are irrelevant, whereas the mass terms are relevant, from the power-counting. The transition between two disordered phases is then described by the non-interacting Dirac point. The nature of the phase boundary between the ordered phase and disordered phases is more difficult to discuss. The critical point at  $m_b = 0$  with  $gN_f \Lambda \neq 0$  can be nevertheless accessible with the large- $N_f$  or  $\epsilon$  expansion ( $4 - \epsilon$  expansion), as we explore in the next section.

### III. LARGE- $N_f$ AND $\epsilon$ EXPANSIONS

#### A. summary of results

In this section, we focus on the nature of the critical point separating the ordered phase and the semi-metallic Dirac phase located at  $m_b = 0$  with  $gN_f \Lambda \neq 0$ . This IR unstable fixed point will be called the GN fixed point. While it is not perturbatively accessible in the coupling constant  $g$ , it can be studied either by the large- $N_f$  expansion or by the  $\epsilon$  expansion.<sup>25-27</sup> The problem of the (2+1)-dimensional Dirac fermions interacting via short-range as well as long-range (Coulombic as well as gauge)

interactions has a long history; in particular, the recent fabrication of graphene, and in particular suspended graphene<sup>28</sup>, motivated many papers to revisit this problem (see for example, Ref. 29).

One of our main focuses in this paper is the effects of four-fermion interactions on the duality relation among order parameters. Of particular interest are the scaling dimensions of the mass bilinears at the GN fixed point associated to the order parameters; we can compare the scaling dimensions of the mass  $\bar{\psi}\psi$  and the mass  $\bar{\psi}\Sigma\psi$ , where the mass matrix  $\Sigma$  corresponds to one of the masses described by  $m_b$  ( $\Sigma \in \gamma^0 \xi_b$  with  $b \in M$ ), and  $\Sigma \notin \{\Sigma_a\}_{a=1, \dots, N_\Sigma}$ . I.e.,  $\Sigma$  is an identity matrix in the Dirac indices, and anticommutes with  $\Sigma_a$  for all  $a = 1, \dots, N_\Sigma$  (i.e., the mass  $\bar{\psi}\Sigma\psi$  is dual to  $\bar{\psi}\Sigma_a\psi$ ), whereas the mass  $\bar{\psi}\psi$  commutes with  $\bar{\psi}\Sigma_a\psi$ .

To leading order in the large- $N_f$  expansion, the anomalous dimension of the fermion field  $\psi$  ( $\eta_\psi$ ), the mass bilinear  $\bar{\psi}\psi$  ( $\eta_{\bar{\psi}\psi}$ ), and the mass bilinear  $\bar{\psi}\Sigma\psi$  ( $\eta_{\bar{\psi}\Sigma\psi}$ ), are given by

$$\begin{aligned} \eta_\psi &= \frac{8 N_\Sigma}{3\pi^2 \tilde{N}}, \\ \eta_{\bar{\psi}\psi} &= \frac{16 N_\Sigma}{3\pi^2 \tilde{N}} (1 + 3) = \frac{64 N_\Sigma}{3\pi^2 \tilde{N}}, \\ \eta_{\bar{\psi}\Sigma\psi} &= \frac{16 N_\Sigma}{3\pi^2 \tilde{N}} (1 - 3) = -\frac{32 N_\Sigma}{3\pi^2 \tilde{N}}, \end{aligned} \quad (17)$$

where we have introduced

$$\tilde{N} := D_\gamma D_\Sigma N_f. \quad (18)$$

Alternatively, we can also look at the anomalous dimensions using the  $\epsilon$  expansion<sup>30,31</sup> (i.e., in  $d = 4 - \epsilon$  dimensions where physical dimension corresponds to  $\epsilon = 1$ ). To leading order in  $\epsilon$ ,

$$\begin{aligned} \eta_\psi &= \frac{1}{2} \frac{\epsilon N_\Sigma}{\tilde{N} + 4 - N_\Sigma}, \\ \eta_{\bar{\psi}\psi} &= \frac{\epsilon N_\Sigma}{\tilde{N} + 4 - N_\Sigma} (1 + 2) = \frac{3\epsilon N_\Sigma}{\tilde{N} + 4 - N_\Sigma}, \\ \eta_{\bar{\psi}\Sigma\psi} &= \frac{\epsilon N_\Sigma}{\tilde{N} + 4 - N_\Sigma} (1 - 2) = \frac{-\epsilon N_\Sigma}{\tilde{N} + 4 - N_\Sigma}. \end{aligned} \quad (19)$$

The calculational details of Eqs. (19) and (17) can be found in the next subsection.

While the results in the large- $N_f$  and the  $\epsilon$  expansions do not match numerically, the signs of the anomalous dimensions agree in both calculations. In particular observe that  $\eta_{\bar{\psi}\psi}$  and  $\eta_{\bar{\psi}\Sigma\psi}$  have opposite sign; the positive/negative sign in these anomalous dimensions directly comes from anticommutation/commutation relations of the masses and order parameters. I.e., the positive/negative sign is a direct manifestation of the duality. To be more precise, observed that in  $\eta_{\bar{\psi}\psi}$  and  $\eta_{\bar{\psi}\Sigma\psi}$  above, two contributions are separately displayed (as seen in “(1 ± 3)” and “(1 ± 2)” in Eqs. (19) and (17), respectively). The first terms in  $\eta_{\bar{\psi}\psi}$  and  $\eta_{\bar{\psi}\Sigma\psi}$

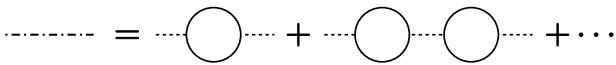


FIG. 2. The boson self-energy in the large- $N_f$  expansion obtained by summing fermion bubbles, where full lines represent the fermion propagator, and broken lines represent the boson propagator.

come from the renormalization of the single fermion field ( $= 2\eta_\psi$ ) and do not know such duality relation, while the second terms have opposite sign (“ $\pm 3$ ” or “ $\pm 2$ ”) for  $\eta_{\bar{\psi}\psi}$  and  $\eta_{\bar{\psi}\Sigma\psi}$  which originates from the anticommutation/commutation relations of the masses and order parameters. Such anticommutation/commutation relations also control presence/absence of topological terms when one integrates the fermionic degrees of freedom to derive the non-linear sigma model (NL $\sigma$ M) (see below).

### B. Large- $N_f$ expansion

We now present some calculational details of the large- $N_f$  and  $\epsilon$ -expansions. In Secs. III B and III C, we first collect diagrammatic calculations for renormalization constants, in the large- $N_f$  and  $\epsilon$ -expansions, respectively. These data will be used in Subsec. III D to compute anomalous dimensions of the fermion field and mass bilinears.

The bare Euclidean action of the  $O(N_\Sigma)$  GN model in terms of the fermionic ( $\psi$ ) and bosonic fields ( $v_a$ ) is Eq. (14):

$$\mathcal{L} = \sum_{\iota=1}^{N_f} \bar{\psi}_\iota (\gamma_\mu \partial_\mu + \sum_{a=1}^{N_\Sigma} v_a \Sigma_a) \psi_\iota + \frac{1}{2g} \sum_{a=1}^{N_\Sigma} v_a^2, \quad (20)$$

where we work in  $d = 3$  space-time dimensions,  $\mu = 1, \dots, d$ .

*a. Boson self-energy* To leading order in the large- $N_f$  expansion, the boson ( $v_a$  field) self-energy is obtained by summing over fermionic bubble diagrams (Fig. 2), leading to the boson propagator

$$\langle v_a^*(\mathbf{k}) v_b(\mathbf{k}') \rangle = \frac{16}{\tilde{N}} \frac{\delta_{ab} \delta_{\mathbf{k}, \mathbf{k}'}}{|k|}, \quad (21)$$

at the non-trivial critical point  $g = g_*$ .

To compute the anomalous dimensions of the fermionic field, as well as the anomalous dimensions of mass terms of different kinds, at the non-trivial critical point, there are three diagrams to be considered: Figs. 3-4.

*b. Fermion self-energy* The diagram corresponding to the Fermion self-energy is shown in Fig. 3. The corre-

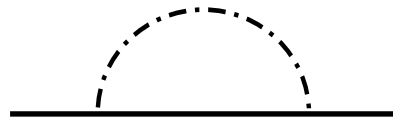


FIG. 3. The fermion self-energy diagram where the broken line represents the boson propagator, Eq. (21).

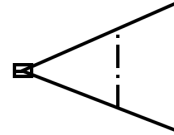


FIG. 4. The vertex correction diagram relevant for the renormalization of the mass bilinear  $\bar{\psi}\psi$  or  $\bar{\psi}\Sigma\psi$ , where the square represents either the insertion of the operator  $\nu\bar{\psi}\psi$  or  $\rho\bar{\psi}\Sigma\psi$ .

sponding integral is:

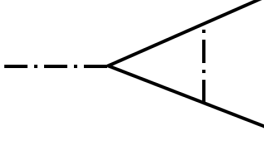
$$\begin{aligned} & \langle \bar{\psi}(\mathbf{q}) \psi(\mathbf{q}) \rangle^{-1} \\ &= i\not{q} + \int \frac{d^3 k}{(2\pi)^3} \frac{i\not{k}}{k^2} \frac{16\Sigma_a \delta_{ab} \Sigma_b}{\tilde{N}|\mathbf{q}-\mathbf{k}|} \\ &= i\not{q} \left[ 1 + \Sigma_\psi^{N_f} \log \left( \frac{\Lambda}{|q|} \right) \right], \end{aligned} \quad (22)$$

where  $\not{k} = k_\mu \gamma_\mu$ , and  $\Sigma_\psi^{N_f} = 16N_\Sigma / (6\pi^2 \tilde{N})$ . In Eq. (22), and from now on, we suppress the flavor index, since correlation functions that consists of several fermionic operators are non-zero only when all fermion fields carry the same flavor index: E.g.,  $\langle \bar{\psi}(\mathbf{q}) \psi(\mathbf{q}) \rangle^{-1} = \langle \bar{\psi}_\iota(\mathbf{q}) \psi_\iota(\mathbf{q}) \rangle^{-1}$  in Eq. (22).

*c.  $\bar{\psi}\psi$  bilinear vertex correction* To compute the anomalous dimension of the fermion bilinear  $\bar{\psi}\psi$ , we add a mass bilinear term  $\nu\bar{\psi}\psi$  to the action, where  $\nu$  is the corresponding “mass”. We also introduce a multiplicative renormalization constant for  $\nu$ ,  $\Delta_\nu^{N_f}$ , in the large- $N_f$  expansion. The vertex diagram corresponding to the renormalization of the mass  $\nu$  is Fig. 4:

$$\begin{aligned} & \Delta_\nu^{N_f} \nu \log \left( \frac{\Lambda}{k} \right) \\ &= \nu \int \frac{d^3 q}{(2\pi)^3} \frac{i(\not{q} + \not{k})}{(q+k)^2} \frac{16\Sigma_a \delta_{ab} \Sigma_b}{\tilde{N}q} \frac{i(\not{q} - \not{k})}{(q-k)^2} \\ &= -\nu \frac{8N_\Sigma}{\pi^2 \tilde{N}} \log \left( \frac{\Lambda}{k} \right). \end{aligned} \quad (23)$$

*d.  $\bar{\psi}\Sigma\psi$  bilinear vertex correction* We now add a term of the form  $\rho\bar{\psi}\Sigma\psi$  to the action. Here, the mass matrix  $\Sigma$  corresponds to one of the masses described by  $m_b$  (i.e.  $\Sigma \in \gamma^0 \xi_b$  with  $b \in M$ ), and  $\Sigma \notin \{\Sigma_a\}_{a=1, \dots, N_\Sigma}$ :  $\Sigma$  is an identity matrix in the Dirac indices, and anti-commutes with  $\Sigma_a$  for all  $a = 1, \dots, N_\Sigma$ . The diagram that determines the renormalization of  $\rho\bar{\psi}\Sigma\psi$  is similar to the one given above (Fig. 4) except for the presence of

FIG. 5. The vertex diagram for  $\lambda$  coupling.

$\Sigma$  matrix:

$$\begin{aligned} & \Delta_\rho^{N_f} \rho \log\left(\frac{\Lambda}{k}\right) \Sigma \\ &= \rho \int \frac{d^3q}{(2\pi)^3} \frac{i(\not{q} + \not{k})}{(q+k)^2} \frac{16\delta_{ab}\Sigma_a\Sigma_b}{\tilde{N}q} \frac{i(\not{q} - \not{k})}{(q-k)^2} \\ &= \rho \frac{8N_\Sigma}{\pi^2\tilde{N}} \log\left(\frac{\Lambda}{k}\right) \Sigma. \end{aligned} \quad (24)$$

### C. $\epsilon$ expansion

The bare Euclidean action  $S = \int d^d r \mathcal{L}$  of the Gross-Neveu-Yukawa model, in terms of the fermionic ( $\psi$ ) and bosonic fields ( $v_a$ ), is given by

$$\begin{aligned} \mathcal{L} &= \sum_{\iota=1}^{N_f} \bar{\psi}_\iota (\gamma_\mu \partial_\mu + \lambda v_a \Sigma_a) \psi_\iota \\ &+ \frac{1}{2} \sum_{a=1}^{N_\Sigma} [(\partial_\mu v_a)^2 + r(v_a)^2] + u \left[ \sum_{a=1}^{N_\Sigma} (v_a)^2 \right]^2. \end{aligned} \quad (25)$$

We now work in  $d = 4 - \epsilon$  space-time dimensions. The bare propagator for the bosonic field  $v_a$  is

$$\langle v_a^*(\mathbf{k}) v_b(\mathbf{k}') \rangle = \frac{\delta_{ab} \delta_{\mathbf{k}, \mathbf{k}'}}{|\mathbf{k}|^2 + r}. \quad (26)$$

To one-loop, we need to consider, for the part of the theory that involves only the bosonic field ( $v_a$ ), the diagrams that appear in renormalizing the  $\phi^4$  theory. In addition, the vertex correction for coupling  $\lambda$ , and the boson self energy correction by a fermion loop need to be calculated.

*e. Vertex correction for coupling  $\lambda$*  The vertex correction of the coupling of the fermionic and bosonic fields  $\lambda$  is given by the following diagram:

$$\begin{aligned} & \Delta_\lambda^\epsilon \lambda \Sigma_a \frac{1}{\epsilon} \\ &= \lambda^3 \int \frac{d^d q}{(2\pi)^d} \frac{\Sigma_b i \not{q} \Sigma_a i(\not{q} - \not{k}) \Sigma_b}{[(q+p_2)^2 + m^2] q^2 (q-k)^2} \\ &= -\frac{2\lambda^3}{(4\pi)^2} \Sigma_a (-N_\Sigma + 2) \frac{1}{\epsilon}. \end{aligned} \quad (27)$$

*f. Boson self energy* The one-loop boson self energy including a fermion loop is given by

$$\begin{aligned} & \langle v_a^*(\mathbf{p}) v_b(\mathbf{p}) \rangle^{-1} \\ &= \delta_{ab} (\mathbf{p}^2 + r) \\ &+ \lambda^2 N_f \int \frac{d^d q}{(2\pi)^d} \text{tr} \left[ \Sigma_a \frac{i \not{q}}{\mathbf{q}^2} \Sigma_b \frac{i(\not{q} + \not{p})}{(\mathbf{q} + \mathbf{p})^2} \right] \\ &= \delta_{ab} (\mathbf{p}^2 + r) + \tilde{N} \frac{\mathbf{p}^2}{2} \int \frac{d^d q}{(2\pi)^d} \frac{\delta_{ab}}{\mathbf{q}^2 (q+p)^2} \\ &= \delta_{ab} (\mathbf{p}^2 + r) + \frac{\tilde{N}}{(4\pi)^2} \frac{\mathbf{p}^2}{\epsilon} \delta_{ab}. \end{aligned} \quad (28)$$

*g. Fermion self-energy* The diagram corresponding to the Fermion self-energy has the same structure as in the large  $N_f$  expansion (Fig. 2) and the corresponding integral is given by

$$\begin{aligned} & \langle \bar{\psi}(\mathbf{k}) \psi(\mathbf{k}) \rangle^{-1} \\ &= i \not{k} + \lambda^2 \int \frac{d^d q}{(2\pi)^d} \frac{i \not{q}}{q^2} \frac{\Sigma_a \delta_{ab} \Sigma^b}{(\mathbf{k} - \mathbf{q})^2 + r} \\ &= i \not{k} \left( 1 + \Sigma_\psi^\epsilon \frac{1}{\epsilon} \right), \end{aligned} \quad (29)$$

where  $\Sigma_\psi^\epsilon = \lambda^2 N_\Sigma / (4\pi)^2$ .

From these three diagrams, we read off the renormalization conditions for the wavefunction renormalizations  $Z_\psi^\epsilon$  and  $Z_v^\epsilon$  for the fermionic ( $\psi$ ) and bosonic ( $v_a$ ) fields, respectively, and for the coupling  $\lambda$  as

$$Z_\psi^\epsilon i \not{p} + \lambda^2 \frac{N_\Sigma}{(4\pi)^2} i \not{p} = \text{finite}, \quad (30)$$

$$Z_v^\epsilon \mathbf{p}^2 + \mathbf{p}^2 \frac{1}{\epsilon} \frac{\tilde{N}}{(4\pi)^2} = \text{finite}, \quad (31)$$

$$m^{-\frac{\epsilon}{2}} \lambda_0 (Z_v^\epsilon)^{\frac{1}{2}} Z_\psi^\epsilon - \frac{2\lambda^3}{(4\pi)^2} \frac{1}{\epsilon} (-N_\Sigma + 2) = \lambda, \quad (32)$$

where we have introduced an arbitrary mass scale  $m \propto \sqrt{r}$ , and  $\lambda_0$  is the bare coupling which does not flow with the mass scale. With the minimal subtraction scheme<sup>27</sup>, these conditions can be used to derive, to one-loop,  $Z_v^\epsilon$  and the beta function for  $\lambda$ ,

$$\begin{aligned} Z_v^\epsilon &= 1 - \frac{1}{\epsilon} \frac{\tilde{N}}{(4\pi)^2}, \\ \beta_{\lambda^2} &:= -m \frac{\partial}{\partial m} \lambda^2 \\ &= -\epsilon \lambda^2 + \frac{2\lambda^4}{(4\pi)^2 \epsilon} \left( \tilde{N}/2 + 4 - N_\Sigma \right), \end{aligned} \quad (33)$$

and also the critical coupling

$$\lambda^{*2} = \frac{8\pi^2 \epsilon}{\tilde{N} + 4 - N_\Sigma}. \quad (34)$$

Below, we will compute the anomalous dimensions of the fermion field and the mass bilinears at the non-trivial

	large- $N_f$ expansion	$\epsilon$ expansion
$\Sigma_\psi^s = \eta_\psi^s$	$\frac{1}{3} \frac{8N_\Sigma}{\pi^2 \tilde{N}}$	$\frac{1}{2} \frac{\epsilon N_\Sigma}{\tilde{N} + 4 - N_\Sigma}$
$\Delta_\nu^s$	$-\frac{8N_\Sigma}{\pi^2 \tilde{N}}$	$-\frac{\epsilon N_\Sigma}{\tilde{N} + 4 - N_\Sigma}$
$\Delta_\rho^s$	$\frac{8N_\Sigma}{\pi^2 \tilde{N}}$	$\frac{\epsilon N_\Sigma}{\tilde{N} + 4 - N_\Sigma}$
$\Delta_\nu^s - \Sigma_\psi^s = \eta_\nu^s$	$\frac{-4}{3} \frac{8N_\Sigma}{\pi^2 \tilde{N}}$	$\frac{-3}{2} \frac{\epsilon N_\Sigma}{\tilde{N} + 4 - N_\Sigma}$
$\Delta_\rho^s - \Sigma_\psi^s = \eta_\rho^s$	$\frac{2}{3} \frac{8N_\Sigma}{\pi^2 \tilde{N}}$	$\frac{1}{2} \frac{\epsilon N_\Sigma}{\tilde{N} + 4 - N_\Sigma}$
$\eta_{\bar{\psi}\psi}^s$	$\frac{8}{3} \frac{8N_\Sigma}{\pi^2 \tilde{N}}$	$\frac{3\epsilon N_\Sigma}{\tilde{N} + 4 - N_\Sigma}$
$\eta_{\bar{\psi}\Sigma\psi}^s$	$\frac{-4}{3} \frac{8N_\Sigma}{\pi^2 \tilde{N}}$	$-\frac{\epsilon N_\Sigma}{\tilde{N} + 4 - N_\Sigma}$

TABLE I. Anomalous dimensions derived from the large- $N_f$  and  $\epsilon$  expansions.

critical coupling  $(\lambda, u) = (\lambda^*, u^*) \neq (0, 0)$ . This fixed point in the Gross-Neveu-Yukawa model is smoothly connected to the GN fixed point.<sup>26,27</sup> As in the large- $N_f$  expansion, we will consider the following three diagrams.

*h.  $\bar{\psi}\psi$  bilinear vertex correction* To compute the anomalous dimensions, we add the mass term  $\nu\bar{\psi}\psi$  to the action, which leads to the vertex diagram of type shown in Fig. 4. It determines, to leading order in  $\epsilon$ , the renormalization constant  $\Delta_\nu^\epsilon$  for the mass term  $\nu\bar{\psi}\psi$  as

$$\begin{aligned} \Delta_\nu^\epsilon \frac{1}{\epsilon} &= \nu \lambda^2 \int \frac{d^d q}{(2\pi)^d} \frac{\Sigma_a \delta_{ab} i \not{q} \Sigma i \not{q} \Sigma_b}{[(\mathbf{q} + \mathbf{k})^2 + m^2] q^2 (q)^2} \\ &= -\nu \frac{2\lambda^2 N_\Sigma}{(4\pi)^2} \frac{1}{\epsilon}. \end{aligned} \quad (35)$$

*i.  $\bar{\psi}\Sigma\psi$  bilinear vertex correction* Similarly, by adding the mass term  $\rho\bar{\psi}\Sigma\psi$  to the action, the renormalization constant  $\Delta_\rho^\epsilon$  for the mass term  $\rho\bar{\psi}\Sigma\psi$  is determined from the vertex diagram of type Fig. 4:

$$\begin{aligned} \Delta_\rho^\epsilon \frac{1}{\epsilon} &= \nu \lambda^2 \int \frac{d^d q}{(2\pi)^d} \frac{\Sigma_a \delta_{ab} i \not{q} \Sigma i \not{q} \Sigma_b}{[(q+p)^2 + m^2] q^2 (q)^2} \\ &= -\rho \frac{2\lambda^2}{(4\pi)^2} \frac{1}{\epsilon} \Sigma_b \Sigma \Sigma_b = \frac{2\lambda^2}{(4\pi)^2} N_\Sigma \rho \Sigma \frac{1}{\epsilon}. \end{aligned} \quad (36)$$

#### D. Renormalization conditions and anomalous dimensions

With diagrammatics in Secs. III B and III C in hand, we can proceed for calculations of anomalous dimensions using minimal subtraction scheme<sup>27</sup>. The renormalization

conditions are given by

$$i\bar{\psi} (Z_\psi^s + \Sigma_\psi^s \mathbf{Div}) = \text{finite}, \quad (37)$$

$$Z_\psi^s \nu_0 + \Delta_\nu^s \mathbf{Div} \nu = \nu, \quad (38)$$

$$Z_\psi^s \rho_0 + \Delta_\rho^s \mathbf{Div} \rho = \rho, \quad (39)$$

where  $s = N_f$  or  $s = \epsilon$  for the large- $N_f$  and  $\epsilon$  expansions;  $\mathbf{Div}$  represents the divergence,  $\mathbf{Div} = \log(\Lambda/k)$  for the large- $N_f$  expansion and  $\mathbf{Div} = 1/\epsilon$  for the  $\epsilon$  expansions;  $\nu_0$  and  $\rho_0$  are the bare masses. We can readily read off the field renormalization  $Z_\psi^s$ , for the fermion field and its anomalous dimension  $\eta_\psi^s$ , as

$$\begin{aligned} Z_\psi^s &= 1 - \Sigma_\psi^s \mathbf{Div}, \\ \eta_\psi^s &= \Sigma_\psi^s. \end{aligned} \quad (40)$$

The dimension  $d_\mathcal{O}$  of an operator  $\mathcal{O}$  at a critical point is defined from the power-law decay of its correlation function as  $\langle \mathcal{O}(\mathbf{r}) \mathcal{O}(\mathbf{0}) \rangle \propto |\mathbf{r}|^{-2d_\mathcal{O}}$ . In  $d = (2+1)$  dimensions, the engineering dimensions of the mass terms  $\bar{\psi}\psi$  and  $\psi\Sigma\psi$  are 2,  $d_{\bar{\psi}\psi}^{(0)} = d_{\psi\Sigma\psi}^{(0)} = 2$ . Accordingly, the engineering dimensions of the masses  $\nu$  and  $\rho$  are 1,  $d_{\bar{\psi}\psi}^{(0)} = d - d_{\bar{\psi}\psi}^{(0)} = 1$  and  $d_{\psi\Sigma\psi}^{(0)} = d - d_{\psi\Sigma\psi}^{(0)} = 1$ .<sup>27</sup>

From the renormalization conditions (39), to leading order in  $N_f$  or in  $\epsilon$ , and in  $d = (2+1)$  dimensions, the anomalous part of the dimensions of the masses  $\nu$  and  $\rho$  can be read off as

$$\eta_\nu^s = \Delta_\nu^s - \Sigma_\psi^s, \quad (41)$$

$$\eta_\rho^s = \Delta_\rho^s - \Sigma_\psi^s. \quad (42)$$

The total dimensions of the masses  $\nu$  and  $\rho$  are then given by  $d_\nu^s = 1 + \eta_\nu^s$  and  $d_\rho^s = 1 + \eta_\rho^s$ . In turn, the dimensions of the fermion bilinears are then given by  $d_{\bar{\psi}\psi}^s = d - d_\nu^s$  and  $d_{\psi\Sigma\psi}^s = d - d_\rho^s$  with the corresponding anomalous dimensions given by  $\eta_{\bar{\psi}\psi}^s = 2d_{\bar{\psi}\psi}^s - 2d$  and  $\eta_{\psi\Sigma\psi}^s = 2d_{\psi\Sigma\psi}^s - 2d$ . These results are summarized in Table I.

## IV. DISCUSSION

*summary of results* Two different order parameters,  $\vec{v}_1$  and  $\vec{v}_2$  are said to be dual to each other when a static defect in one of them traps a quantum number (or ‘‘charge’’) of the other. In this paper, we have discussed the interaction effects on such a pair of order parameters. The complementary nature of the pair of the order parameters shows up also in their dynamical properties (correlation functions) in the following sense: When a quantum phase transition is driven by fluctuations in one of the order parameter,  $\vec{v}_1$ , say, approaching the transition from the disordered (paramagnetic) side, the order parameter correlation at the critical point is reduced. On the other hand, such fluctuations enhance the correlation of the order parameter  $\vec{v}_2$ , which is dual to  $\vec{v}_1$ .

If we can experimentally monitor, at a given quantum critical point, the correlation functions of a pair of

such order parameters, the complementary relationship (duality) can be revealed by extracting their anomalous dimensions, which can, at the same time, be helpful to identify the main driving forces of the transition, as discussed above. For example, for the Néel and VBS order parameters which can compete with each other around a quantum critical point, the neutron scattering experiment can detect the Néel order, whereas the scanning tunneling spectroscopy measurement can extract some information on the VBS order. Another probe which can potentially be used to detect the correlation of the VBS order parameter is its coupling to phonons. As a consequence of such coupling, information on the VBS correlation can be extracted by looking at the imaginary part of the phonon response function<sup>32</sup> using, say, X-ray scattering. Similar method has been used to identify fluctuations in the dimer order parameter in spin-chains which go through spin-Peierls transition.<sup>33</sup>

We, again, emphasize that the type of competitions among order parameters discussed in this paper has a topological origin, rather than some accidental energetic reasons, and hence is largely independent of microscopic details of the system. Whether or not such duality relationship among correlation functions holds beyond Dirac systems that we discussed in terms of the large- $N_f$  and  $\epsilon$  expansions, should further be studied in future. For example, numerical study in the  $J-Q$  model<sup>22</sup> would be promising in this regard.

*description in terms of the NL $\sigma$ M* To further illustrate the topological origin behind the duality, let us seek for an alternative description of fluctuating order parameters. Instead of taking the non-interacting Dirac fermions as a starting point, consider the system which is deep inside the ordered phase (the large- $gN_f$  region in Fig. 1). It is then reasonable to employ a description in terms of the fluctuating but non-vanishing order parameter. The dynamics of the order parameter may be described by the  $O(N_\Sigma)$  NL $\sigma$ M whose kinetic term is given by, the following imaginary time action

$$S_{\text{NL}\sigma\text{M}} = \frac{1}{t} \int d^3x \partial_\mu n_a \partial_\mu n_a \quad (43)$$

where  $\sum_{a=1}^{N_\Sigma} n_a^2 = 1$  [see Eq. (15)], and  $t$  is the coupling constant of the NL $\sigma$ M. Such NL $\sigma$ M description can be derived, inside the ordered phase, by integrating over gapped fermions in the presence of slowly varying order parameter field  $\vec{v}_1$ <sup>34</sup>. The NL $\sigma$ M is in the weak coupling regime (small  $t$ ) when  $g$  (in Eq. 5, say) is large, while it is in the strong coupling regime (large  $t$ ) when  $g$  approaches the critical coupling  $g_*$  from the disordered side.

In addition to the NL $\sigma$ M kinetic term, the integration over fermions gives rise to either the Wess-Zumino-Witten (WZW)-term,  $\theta$ -term, or the Berry phase term in the NL $\sigma$ M (for alternative derivation of topological terms see Ref. 35). For example, when we are in the  $O(4)$  ordered phase, the NL $\sigma$ M is supplemented with the

$\theta$ -term,

$$S_\theta = i \frac{\theta}{2\pi^2} \int d^3x \epsilon_{abcd} n_a \partial_\tau n_b \partial_x n_c \partial_y n_d. \quad (44)$$

Here, the  $\theta$  angle can be computed from the microscopic Dirac model<sup>34</sup>,

$$\frac{\theta}{\pi} = 1 - \frac{9}{8} \cos \varphi + \frac{1}{8} \cos 3\varphi, \quad (45)$$

where  $\varphi$  is determined from the ratio between the amplitude of the  $O(4)$  order parameter (as defined in Sec. II B) and the mass term,  $\tan \varphi = -|\mathbf{v}|/m_3$ : When fermions are gapped solely because of the  $O(4)$  order parameter (i.e.  $m_3 = 0$ )  $\mathbf{v} = |\mathbf{v}|\mathbf{n}$ , which develops a finite expectation value in the  $O(4)$  ordered phase,  $\theta = \pi$ . On the other hand, for example, if we add a mass term  $m_3 \bar{\psi} \Sigma_3 \psi$  in the ordered phase, which anticommutes with the  $O(4)$  order parameter  $v_a \bar{\psi} \Sigma_a \psi$ , the  $\theta$ -term deviates from  $\theta = \pi$ .

Following the spirit of the Goldstone-Wilczek formula<sup>36</sup>, when the order parameters are treated as a static background, we can see that it is the  $\theta$ -term which implements the duality within the NL $\sigma$ M field theory. When this operator acquires an expectation value, the VBS order results. In this manner the NL $\sigma$ M field theory contains the ingredients describing both the ordered and paramagnetic phases. This is in fact in line with the known fact that the Berry phase term in the (2+1) dimensional  $O(3)$  NL $\sigma$ M secretly encodes the VBS order, and that in the paramagnetic phase the presence of the Berry phases leads to the VBS order.<sup>21,37</sup>

*speculation on the criticality and the RG flow of the NL $\sigma$ M with  $\theta$  term*

Having established the duality relation within the ordered phase of the NL $\sigma$ M, it is now interesting to ask what would happen when we approach the strongly coupled region where the order parameter fluctuations are strong. In particular, how does the RG flow of the  $O(4)$  NL $\sigma$ M with  $\theta$ -term look like? The relevance of the topological terms ( $\theta$ -term as well as other topological terms such as the Wess-Zumino-Witten term) in the NL $\sigma$ M to the deconfined quantum criticality has been discussed in Refs. 34, 38, and 39. (See also a recent paper 40).

Unfortunately, the role of the topological term on the quantum criticality in (2+1)-dimensions is not well-understood. This situation should be contrasted with the state of our understanding on the  $\theta$ -term in the  $O(3)$  NL $\sigma$ M in (1+1)-dimensions; Starting from the Haldane conjecture, it is by now well-known that the different nature of the ground states of the  $S = \text{integer}$  and  $S = \text{half-odd integer}$  spin chain is reflected to the value of the  $\theta$ -term,  $\theta = 2\pi \times S \pmod{2\pi}$  in the  $O(3)$  NL $\sigma$ M. Quite surprisingly, in (1+1)-dimensions, the integrability of the  $O(3)$  NL $\sigma$ M allows us to “prove” that the  $O(3)$  NL $\sigma$ M at  $\theta = \pi$  flows, in the RG sense, into a gapless critical point (the  $SU(2)$  Wess-Zumino-Witten theory at level one). The low-lying excitation at the critical point consists, not of magnons, but (fermionic) spinons. When detuned from  $\theta = \pi$  (by breaking a link parity symmetry,

say, with bond dimerization in the Heisenberg exchange coupling), the  $\theta$ -term flows to 0 or  $2\pi$ , where a system is in a gapped paramagnetic phase.

We now present some speculations on the effect of the topological term in (2+1) dimensions in the region when the fluctuations of the NL $\sigma$ M order parameter is strong. Let us start from the ordered phase of the NL $\sigma$ M; it exists for the small NL $\sigma$ M coupling,  $t \ll 1$ , and this should be true for any value of  $\theta$ . As we crank up the NL $\sigma$ M coupling constant  $t$ , the interactions between “magnons” become stronger. It would then seem reasonable to assume that, even in the presence of non-vanishing  $\theta$ , we reach a critical point by eventually destroying the (long-range) order, at which the NL $\sigma$ M order parameter develops a critical (power-law) correlation with vanishing expectation value,  $\vec{v} = 0$ .

Recall that in the conventional NL $\sigma$ M without any topological term, the nature of such transition can be captured by e.g. the  $2 + \epsilon$  expansion. On the other hand if we stay exactly in three space-time dimensions, which is necessary if we are after the effect of the topological term, the NL $\sigma$ M is not perturbatively renormalizable (although it may be renormalizable in terms of the non-perturbative RG). It should be considered as an effective field theory, and is not UV complete. As we approach the putative quantum critical region (the strong coupling region of the NL $\sigma$ M) described above, the NL $\sigma$ M description should be replaced by some other description. The question then is, to which extent we can deduce such UV (high-energy) description for the case of non-vanishing  $\theta$ .

In terms of the corresponding fermionic model Sec. II B, which should be regarded as a more microscopic (or UV) description, increasing  $t$  (the coupling constant of the NL $\sigma$ M) corresponds to reducing the four fermion coupling constant  $g$ . In terms of the fermionic phase diagram (Fig. 1), we thus approach the phase boundary from the ordered side. In particular,  $|\mathbf{v}| = 0$  corresponds to the case of  $\theta = 0$ , and in this case, we approach the GN critical point separating the ordered phase and paramagnetic phase (Dirac semi-metal phase). One would then conclude that a UV critical point of the NL $\sigma$ M at  $\theta = \pi$ , if exists, would correspond to the GN fixed point.

This is a tempting, but of course very dangerous, argument. We would, however, expect, by matching with the fermionic description, the following: at the UV critical point of the NL $\sigma$ M at  $\theta = \pi$ , not only the NL $\sigma$ M order parameter develops critical correlation, but its dual order parameter also does so. (These order parameters are called  $\vec{v}_1$  and  $\vec{v}_2$  in the beginning of this section). This is,

of course, a complete surprise from the NL $\sigma$ M point of view: There is no inkling of  $\vec{v}_2$  order parameter whatsoever in the ordered phase, and controlling coupling constant of the NL $\sigma$ M ( $t$  in Eq. 43) has nothing to do with  $\vec{v}_2$  order. Nevertheless because of the  $\theta$ -term, making  $t$  large (destabilizing the order parameter  $\vec{v}_1$ ) somehow makes  $\vec{v}_2$  correlation stronger, since the  $\vec{v}_2$  order parameter within the NL $\sigma$ M is realized as a defect in the  $\vec{v}_1$  parameter. This is in fact in line with the non-trivial identification of the VBS order parameter as the skyrmion creation operator in the (2+1) dimensional O(3) NL $\sigma$ M augmented with the Berry phase term.<sup>21,37</sup> The VBS phase arises as a proliferation of monopoles in the presence of non-trivial Berry phases. Thus, while the more precise nature of the putative quantum critical point at  $\theta = \pi$  is difficult to study, overall physical picture related to the physics of  $\theta$ -term seems to be inferred from the fermionic GN model description.

Another interesting issue is the RG flow which incorporates both  $t$  and  $\theta$  (the couplings of kinetic and topological terms in the NL $\sigma$ M). In the weakly coupled region ( $t/\Lambda \ll 1$ ), the presence of the non-vanishing  $\theta$  little affects the RG flow, while this may not be the case in the strongly coupled region ( $t/\Lambda \simeq 1$ ). In fact, this is the case for the NL $\sigma$ M on the Grassmannian manifold in two dimensions, which is relevant to the two parameter scaling flow of the quantum Hall effect.<sup>41</sup> Again by matching the NL $\sigma$ M description with the fermionic GN model description, since the  $\theta$ -term is correlated to the mass term  $m_b\psi\Sigma_b\psi$  (see Eq. 45), it would be then interesting to “guess” the RG flow of the  $\theta$ -term from the RG flow of the mass term. Within the large- $N_f$  or  $\epsilon$  expansion, the scaling dimension of the fermion mass  $m_b\psi\Sigma_b\psi$  at the GN critical point is very close to the scaling dimension at the trivial (non-interacting Dirac) fixed point. Thus, when  $1/N_f$  or  $\epsilon$  is small enough, the mass term is a relevant perturbation to the GN fixed point, and it grows under the RG. This would suggest the  $\theta$ -term is also relevant in the strong coupling region of the NL $\sigma$ M at  $\theta = \pi$ ; the deviation of the  $\theta$ -angle from  $\theta = \pi$  grows under the RG. However, in principle, more exotic possibility, i.e., the  $\theta$ -term at the non-trivial critical point being irrelevant, can also be realized. We leave these issues for future studies.

## ACKNOWLEDGMENTS

We would like to thank D. H. Lee for insightful discussions. SR thanks the Center for Condensed Matter Theory at University of California, Berkeley for its support. PG acknowledges funding from LBNL DOE-504108.

<sup>1</sup> K. S. Novoselov, A. K. Geim, S. V. Morozov, D. Jiang, M. I. Katsnelson, I. V. Grigorieva, S. V. Dubonos, and A. A. Firsov, Nature **438**, 197 (2005).

<sup>2</sup> Y. Zhang, Y. B. Zhang, Y. W. Tan, H. L. Stormer, and P. Kim, Nature **438**, 201 (2005).

<sup>3</sup> M. Z. Hasan and C. L. Kane, Rev. Mod. Phys. **82**, 3045 (2010).

- <sup>4</sup> D. Hsieh, D. Qian, L. Wray, Y. Xia, Y. Hor, R. Cava, and M. Hasan, *Nature* **452**, 970 (2008).
- <sup>5</sup> D. Hsieh, D. Qian, L. Wray, Y. Xia, Y. Hor, R. Cava, and M. Hasan, *Science* **323**, 919 (2009).
- <sup>6</sup> Y. Xia, D. Qian, D. Hsieh, L. Wray, H. Pal, H. Lin, A. Bansil, D. Grauer, Y. S. Hor, R. J. Cava, and H. M. Z, *Nature Phys.* **5**, 398 (2009).
- <sup>7</sup> D. Hsieh, Y. Xia, D. Qian, L. Wray, H. J. Dil, F. Meier, J. Osterwalder, L. Patthey, J. G. Checkelsky, N. P. Ong, A. V. Fedorov, H. Lin, A. Bansil, D. Grauer, Y. S. Hor, R. J. Cava, and M. Z. Hasan, *Nature* **460**, 1101 (2009).
- <sup>8</sup> A. Kobayashi, S. Katayama, K. Noguchi, and Y. Suzumura, *J. Phys. Soc. Jpn.* **73**, 3135 (2004).
- <sup>9</sup> A. Kobayashi, S. Katayama, K. Noguchi, and Y. Suzumura, *J. Phys. Soc. Jpn.* **75**, 054705 (2006).
- <sup>10</sup> C.-Y. Hou, C. Chamon, , and C. Mudry, *Phys. Rev. Lett.* **98**, 186809 (2007).
- <sup>11</sup> K. Nomura, S. Ryu, and D.-H. Lee, *Phys. Rev. Lett.* **103**, 216801 (2009).
- <sup>12</sup> G. W. Semenoff, *Phys. Rev. Lett.* **53**, 2449 (1984).
- <sup>13</sup> F. D. M. Haldane, *Phys. Rev. Lett.* **61**, 2015 (1988).
- <sup>14</sup> I. H. Herbut, *Phys. Rev. Lett.* **99**, 206404 (2007).
- <sup>15</sup> P. Ghaemi, S. Ryu, and D.-H. Lee, *Phys. Rev. B* **10**, 3235 (2010).
- <sup>16</sup> P. Ghaemi and F. Wilczek, (2007), arXiv:0709.2626.
- <sup>17</sup> L. Santos, S. Ryu, C. Chamon, and C. Mudry, *Phys. Rev. B* **82**, 165101 (2010).
- <sup>18</sup> D. L. Bergman and K. Le Hur, *Phys. Rev. B* **79**, 184520 (2009).
- <sup>19</sup> S. Ryu, C. Mudry, C.-Y. Hou, and C. Chamon, *Phys. Rev. B* **80**, 205319 (2009).
- <sup>20</sup> P. Hosur, S. Ryu, and A. Vishwanath, *Phys. Rev. B* **81**, 045120 (2010).
- <sup>21</sup> T. Senthil, A. Vishwanath, L. Balents, S. Sachdev, and M. P. A. Fisher, *Science* **303**, 1490 (2004).
- <sup>22</sup> A. W. Sandvik, *Phys. Rev. Lett.* **98**, 227202 (2007).
- <sup>23</sup> R. K. Kaul, R. G. Melko, M. A. Metlitski, and S. Sachdev, *Phys. Rev. Lett.* **101**, 187206 (2009).
- <sup>24</sup> D. J. Gross and A. Neveu, *Phys. Rev. D* **10**, 3235 (1974).
- <sup>25</sup> S. Hands, A. Kocic, and J. B. Kogut, *Annals of Physics* **224**, 29 (1993).
- <sup>26</sup> M. Moshe and J. Zinn-Justin, *Phys.Rept.* **385**, 69 (2003).
- <sup>27</sup> J. Zinn-Justin, *Quantum Field Theory and Critical Phenomena* (Oxford University Press, 1993).
- <sup>28</sup> X. Du, I. Skachko, A. Barker, and E. Y. Andrei, *Nature Nanotechnology* **3**, 491 (2008).
- <sup>29</sup> V. N. Kotov, B. Uchoa, V. M. Pereira, A. H. C. Neto, and F. Guinea, arXiv:1012.3484 (2010).
- <sup>30</sup> L. Balents, M. P. A. Fisher, and C. Nayak, *Int. J. of Mod. Phys. B* **12**, 1033 (1998).
- <sup>31</sup> P. Ghaemi and T. Senthil, *Phys. Rev. B* **73**, 054415 (2005).
- <sup>32</sup> M. C. Cross and D. S. Fisher, *Phys. Rev. B* **19**, 402 (1979).
- <sup>33</sup> E. T. Abel, K. Matan, F. C. Chou, E. D. Isaacs, D. E. Moncton, H. Sinn, A. Alatas, and Y. S. Lee, *Phys. Rev. B* **76**, 214304 (2007).
- <sup>34</sup> A. Tanaka and X. Hu, *Phys. Rev. Lett.* **95**, 036402 (2005).
- <sup>35</sup> H. Yao and D.-H. Lee, (2010), arXiv:1003.2230.
- <sup>36</sup> J. Goldstone and F. Wilczek, *Phys. Rev. Lett.* **47**, 986 (1981).
- <sup>37</sup> T. Senthil, L. Balents, S. Sachdev, A. Vishwanath, and M. P. Fisher, *Phys. Rev. B* **70**, 144407 (2004).
- <sup>38</sup> A. Tanaka and X. Hu, *Phys. Rev. B* **74**, 140407 (2006).
- <sup>39</sup> T. Senthil and M. P. A. Fisher, *Phys. Rev. B* **74**, 064405 (2006).
- <sup>40</sup> C. Xu and A. W. W. Ludwig, (2011), arXiv:1112.5303.
- <sup>41</sup> R. E. Prange and S. M. Girvin, *The Quantum Hall Effect* (Springer, 1987).